A Rationally Designed Turn-Helix Peptide

M. Dhanasekaran,† F. Fabiola,‡ V. Pattabhi,‡ and S. Durani*,†

Department of Chemistry and Biotechnology Center, Indian Institute of Technology Bombay Mumbai-400 076, and Department of Crystallography and Biophysics, University of Madras, Chennai-600 025, India

Received December 8, 1998
Revised Manuscript Received April 9, 1999

Protein folding, according to the framework model, is initiated in elements of locally ordered peptide structure that can serve as nucleators and direct the ordering of connected peptide segments into particular kinds of higher order motifs.[1] A minimalist approach to complex motifs could thus use simple peptide folds as conformation nucleators. A recurrent higher order motif in proteins has a helix or a β-strand connected to a turn that is the intermotif linker in such complex motifs as "helix-turn-helix" and "strand-turn-helix". Among intermotif linkers, γ- and β-turns are the simplest[2] and could be promising nucleators usable in de novo design. In fact, β-hairpin, a "strand-turn-strand" motif, was designed successfully by using a type II′ β-turn as the nucleator.[3] For a similar approach to the "turn-helix" motif, the type I, I′, II, or II′ β-turns, the natural intermotif linkers in contrast with the type III β-turn that is a natural helix nucleator, could be exploited as the artificial helix nucleators. The type II and II′ β-turns have sequence chiralities that make them particularly facile targets for de novo design.[4] We have successfully accomplished the exploitation of the type II′ β-turn as a helix nucleator.[5] The pentapeptide Boc-Val-Pro-(D)Asp-Asp-Val-OMe was more recently reported from our lab as a consecutive β-turn, combining a type II β-turn and an Asx[6] turn that had C-terminal geometry that made it a potential helix nucleator.[7] Modifications and extensions with helicogenic residues, including the stereochemically constrained Aib, furnish the octapeptide Boc-Val-Pro-(D)Asp-Aib-Leu-Aib-Leu-Ala-NHMe as a potential turn-helix motif. Solution-phase synthesis[8] followed by NMR and crystal structure characterization establish that, indeed, the octapeptide is a turn-helix motif with the segment Boc-Val(1)-Pro(2)-(D)Asp(3)-Aib(4) in type II β-turn conformation and the segment Aib(4)-Leu(5)-Aib(6)-Leu(7)-Ala-(8)-NHMe as an overlapping 3_{10} helix in which (D)Asp is the N-cap residue and the putative helix folding nucleator.

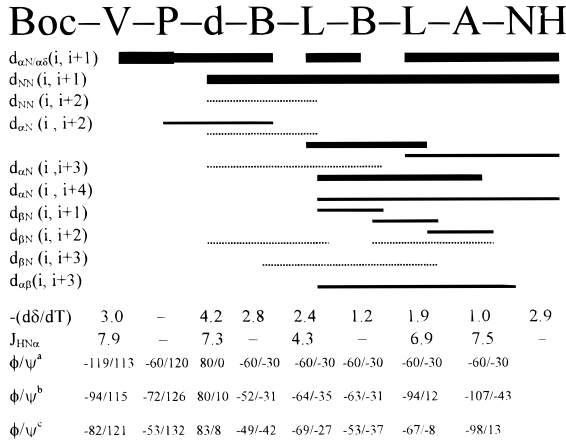

-(dδ/dT)	3.0	–	4.2	2.8	2.4	1.2	1.9	1.0	2.9
$J_{HN\alpha}$	7.9	–	7.3	–	4.3	–	6.9	7.5	–
ϕ/ψ^a	-119/113	-60/120	80/0	-60/-30	-60/-30	-60/-30	-60/-30	-60/-30	
ϕ/ψ^b	-94/115	-72/126	80/10	-52/-31	-64/-35	-63/-31	-94/12	-107/-43	
ϕ/ψ^c	-82/121	-53/132	83/8	-49/-42	-69/-27	-53/-37	-67/-8	-98/13	

[a]The standard values[1,6], with Val(1) in extended parallel β-sheet conformation.
[b]The conformer with lowest energy from simulated annealing molecular dynamics.
[c]The conformer in crystal state.

Figure 1. Summary of NOEs, temperature coefficients (ppb/K), $J_{NH\alpha}$ (Hz), and ϕ and ψ dihedral angles (deg). The line thicknesses are in proportion to the relative NOE intensities.

Short peptides are ideally characterized by NMR, and among NMR observables, NOEs tend to be the most informative of the conformational states sampled.[9] Only eight amide resonances could be observed in the octapeptide dissolved in DMSO,[10] and hence only one of two possible isomers across the Val(1)−Pro-(2) amide bond is populated. An NOE between Val(1)C^{α}H and Pro(2)C^{δ}H established that the observed isomer is in trans-amide geometry. This is in conformity with the reports that the trans isomer predominates when β-branched Val precedes Pro.[1b,4b] Several intra- and interresidue NOEs were observed in the ROESY[11] spectrum of the octapeptide in DMSO, and infact, the NOE density was the largest reported for any peptide of comparable length to the best of our knowledge. Several important NOEs, classified as very strong, strong, medium, weak, and very weak relative to the intensity of ROESY, cross-peak between Pro-(2) δ protons, are presented in Figure 1 as lines, of thickness proportional to the relative cross-peak volumes. Although several potential NOEs are unobservable due to resonance overlaps and to the occurrence of Aib which lacks the α proton, the density as well as intensity of NOEs suggest that either a single folded conformer is populated or a few rapidly interconvertible folded conformers are populated that have short distances between several far-off protons. Even if an ensemble of conformers is

* To whom correspondence should be addressed. Fax: 91−022−578 3480. E-mail: sdurani@btc.iitb.ernet.in.
† Indian Institute of Technology.
‡ University of Madras.

(1) Kim, P. S.; Baldwin, R. L. *Annu. Rev. Biochem.* **1982**, *51*, 459−489. (b) Dyson, H. J.; Rance, M.; Houghten, R. A.; Lerner, R. A.; Wright, P. E. *J. Mol. Biol.* **1988**, *201*, 161−200. (c) Baldwin, R. L. *Trends Biochem. Sci.* **1989**, *14*, 291−294. (d) Scholtz, J. M.; Baldwin, R. L. *Annu. Rev. Biophys. Biomol. Struct.* **1992**, *21*, 95−118. (e) Krplus, M.; Weaver, D. L. *Protein Sci.* **1994**, *3*, 650−668. (f) Baldwin, R. L. *J. Biomol. NMR* **1995**, *5*, 103−109. (g) Alba de, E.; Blanco, F. J.; Jimenez, M. A.; Rico, M.; Nieto, J. L. *Eur. J. Biochem.* **1995**, *233*, 283−292.

(2) Chou, P. Y.; Fasman, G. D. *J. Mol. Biol.* **1977**, *115*, 135−175. (b) Wilmot, C. M.; Thornton, J. M. *J. Mol. Biol.* **1988**, *203*, 221−232. (c) Hutchinson, E. G.; Thornton, J. M. *Protein Sci.* **1994**, *3*, 2207−2216.

(3) Ramirez-Alvarado, M.; Blanco, F. J.; Niemann, H.; Serrano, L. *J. Mol. Bio.* **1997**, 273, 898−912. (b) Maynard, A. J.; Sharman, G. J.; Searle, M. S. *J. Am. Chem. Soc.* **1998**, *120*, 1996−2007. (c) Stanger, H. E.; Gellman, S. *J. Am. Chem. Soc.* **1998**, *120*, 4236−4237. (d) Das, C.; Raghothama, S.; Balaram, P. *J. Am. Chem. Soc.* **1998**, *120*, 5812−5813.

(4) Rose, G. D.; Gierasch, L. M.; Smith, J. A. *Adv. Protein Chem.* **1985**, *37*, 1−109. (b) Imperiali, B.; Fisher, S. L.; Moats, R. A.; Prins, T. J. *J. Am. Chem. Soc.* **1992**, *114*, 3182−3188. (c) Struthers, M. D.; Cheng, R. P.; Imperiali, B. *Science* **1996**, *271*, 342−344.

(5) Bobde, V.; Beri, S.; Durani, S. *Tetrahedron* **1993**, *49*, 5397−5406. (b) Bobde, V.; Sasidhar, Y. U.; Durani, S. *Int. J. Pept. Protein Res.* **1994**, *46*, 209−218. (c) Bobde, V.; Beri, S.; Rawale, S.; Satyanarayana, V.; Durani, S. *Tetrahedron* **1995**, *51*, 3077−3086.

(6) The abbreviations used: Aib, α-aminoisobutyric acid; Boc, *tert*-butyloxycarbonyl; NOE, nuclear Overhauser effect; ROESY, rotating frame nuclear Overhauser enhancement spectroscopy; DMSO, dimethyl sulfoxide; Asx, the amino acids Asp and Asn.

(7) Fabiola, F.; Pattabi, V.; Raju, E. B.; Durani, S. *J. Pept. Res.* **1997**, *50*, 352−356.

(8) The peptide synthesis was by solution-phase methodology, and the purification of final peptide was by RP-HPLC on a C-18 column eluting with CH_3CN water. Bodanszky, M.; Bodanszky, A. *The Practice of Peptide Synthesis*; Springer-Verlag: NewYork, 1984.

(9) Wuthrich, K. *NMR of Proteins and Nuclic Acids*; Wiley: New York, 1986.

(10) Val(1)NH, (D)Asp(3)NH, Aib(4)NH, Leu(5)NH, Aib(6)NH, Leu(7)-NH, Ala(8)NH, and N*H*Me.

(11) NMR measurements were in DMSO-d_6 on a Bruker AM 500 spectrometer with a 10mM peptide solution which showed no chemical shift or line-width variation on a 10-fold dilution and, hence, absence of any noticeable intermolecular aggregation. Resonance assignments were with combined use of TOCSY and ROESY spectra. The ROESY spectra were recorded with a mixing time of 250 ms. The variable-temperature experiments to record the temperature coefficients were at 5° intervals in the range 25−50 °C. (a) Jeener, J.; Meier, B. H.; Bachmann, P.; Ernst, R. R. *J. Chem. Phys.* **1979**, *71*, 4546−4553. (b) Bax, A.; Davis, D. G. *J. Magn. Reson.* **1985**, 63, 207−213. (c) Davis, D. G.; Bax A. *J. Am. Chem. Soc* **1985**, *107*, 2821−2823. (d) Rance, M. *J. Magn. Reson.* **1987**, *65*, 2821−2823.

10.1021/ja984237v CCC: $18.00
Published on Web 05/29/1999

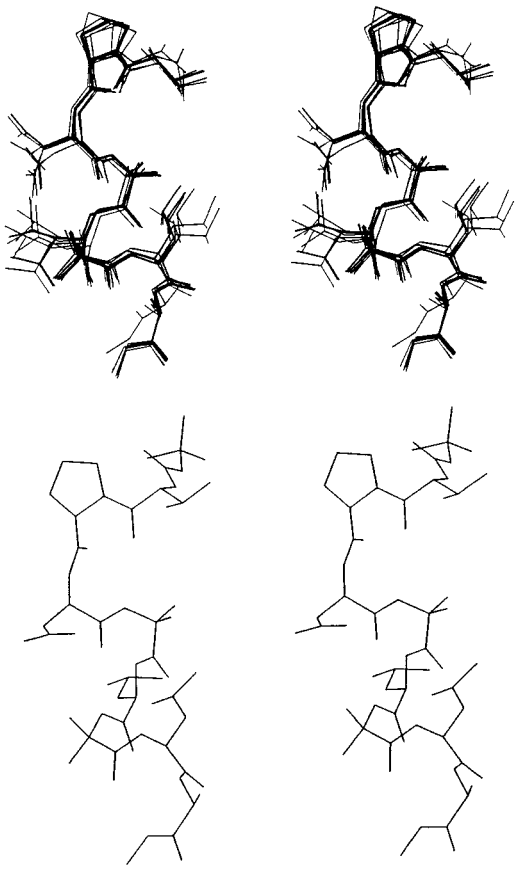

Figure 2. Stereodiagrams representing conformers populated in solution (upper panel) according to NOE restrained simulated annealing molecular dynamics and observed in crystal state (lower panel), showing only the backbone traces. Ten randomly selected low-energy structures are overlaid in the upper panel.

assumed, the dominant conformer certainly has its segment Aib-(4)-Ala(8)NHMe in helical conformation, because the helical signature of sequential $d_{NN}(i, i + 1)$ NOEs and nonsequential $d_{\alpha N}$-$(i, i + 2)$, $d_{NN}(i, i + 2)$, $d_{\alpha N}(i, i + 3)$, $d_{\alpha\beta}(i, i + 3)$, $d_{\beta N}(i, i + 3)$, and $d_{\alpha N}(i, i + 4)$ NOEs, spanning the segment (D)Asp(3)-Ala-(8), is observed as noted in Figure 1. A simulated annealing molecular dynamics analysis,[12] performed with 8 intraresidue and 26 interresidue distance restraints derived from the NOEs,[13] was found to converge to a single family of conformers regardless of the starting structure. The rms deviation of the backbone atoms of all the final conformers was <0.6 Å over the structure averaged over all the conformers populated. Ten randomly selected low-energy conformers superimposed in Figure 2 are all noted to be type II β-turn initiated 3_{10} helices with several NHs H-bonded to the backbone C═Os. This is in conformity with the intramolecularly H-bonded nature of several amide protons as suggested by the amide temperature coefficients less than -0.3 ppb/K[9,14] (Figure 1). Many of the $J_{NH\alpha}$ values are observed to be larger than those expected of a 3_{10} helix, and hence, the molecular ensemble in solution could include conformers in which the peptide backbone is in extended or random conformation. However, the conformer in crystal state quite clearly is the turn-helix motif.[15] The torsional angles as well as the H-bonds in crystal state characterize a type II β-turn in segment Val(1)-Pro-(2)-(D)Asp(3)-Aib(4) and an overlapping 3_{10} helix in segment Aib(4)-Ala(8)-NHMe (Figure 1) for which (D)Asp is the N-cap residue. The ϕ,ψ angles of the lowest energy conformer from molecular dynamics analysis and of the crystal state conformer are in good agreement with the ideal angles for both type II β-turn and 3_{10} helix.[16] An interesting deviation, however, is in that the ϕ,ψ angles of Aib(4) in both crystal and solution state are observed to be closer to the standard α-helical angles than to 3_{10} angles. Participation of the Aib in both the type II β-turn, donating an H-bond to Val(1) C═O, and the 3_{10} helix, accepting an H-bond from Leu(7) NH, could influence its ϕ,ψ angles. The $i \rightarrow i + 2$ type H bonding of (D)Asp(3) carboxylate with Leu(5) NH could be the interaction nucleating the helix folding. The diminished temperature coefficient of Leu(5) NH, suggesting its solvent-shielded nature, is in accordance with possible participation of the NH in helix nucleation. Its potentially helix nucleating H bonding with (D)Asp(3) carboxylate was found to be also operative in at least 50% of the energy-minimized structures in the molecular dynamics analysis. Asn followed by Asp are the most favored N-cap residues in protein helices forming $i \rightarrow i + 2$ or $i \rightarrow i + 3$ type H bonds with main chain NHs, and could be the nucleators responsible for helix folding.[17] The exploitation of (D)Asp as the nucleator of both type II β-turn and 3_{10} helix is the cornerstone of the de novo design accomplished in this study. The extended conformation of Val(1) in both solution and crystal state (Figure 1) makes it a favorable attachment point for a connected motif, leading toward possible elaboration of even more complex higher order motifs in the future.

Acknowledgment. The project funding was from Department of Science and Technology and Department of Atomic Energy, Government of India. The use of the NMR facility at National High Field NMR Facility, TIFR, Mumbai is most gratefully acknowledged. M.D. and F.F. acknowledge financial support from CSIR.

Supporting Information Available: ^{1}H NMR, 2D TOCSY, and 2D ROESY spectra, distance restraints used in molecular dynamics calculation, and X-ray structural information. This material is available free of charge via the Internet at http://pubs.acs.org.

JA984237V

(12) Molecular dynamics simulation was with INSIGHT/DISCOVER package (Biosym Technologies, San Diego, CA). A distance-dependent dielectric constant ($2.5r$ where r is distance in Å) was used, and Asp was assumed to be always in charged form. All hydrogens were treated explicitly, and all ω dihedrals were constrained as trans by a 100 kcal/rad energetic penalty. Distance constraint with a force constant of 25 kcal/mol was applied in the form of a flat-bottom potential well with a common lower bound of 2.0 Å and an upper bound of 2.5, 3.0, 3.5, 4.0, or 4.5 Å, in accordance with the NOE intensity. The starting structures minimized with all restraints in place, first with steepest descent and then with conjugate gradient algorithm, were subjected to simulated annealing. A two hundred picosecond MD run at 1000 K was followed by cooling to 300 K in 7 steps for a total of 35 ps, and then steepest descent and conjugate gradient minimization. One hundred final energy minimized structures were sampled at 2 ps intervals.

(13) Interproton distance restraints were generated from the integrals of ROESY cross-peak volumes, using a reference distance of 1.85 Å for Pro δ protons. No stereospecific assignments were made and, hence,, pseudo atom corrections were applied for all diastereotopic protons when imposing the NOE restraints. Wuthrich, K.; Billeter, M.; Braun, W. *J. Mol. Biol.* **1983**, *169*, 949−961.

(14) $d\delta/dT$ values of <-3 ppb/K are typical for solvent-shielded NHs and >-4ppb/K are typical for solvent-exposed NHs. Kessler, H. *Angew. Chem., Int. Ed. Engl.* **1982**, *21*, 512−523.

(15) Colorless rectangular crystals ($3 \times 2 \times 2$ mm) were obtained by slow evaporation from a dimethylformamide solution and were used for intensity data collection on an Enarf-Nonius CAD4 diffractometer with CuKα(λ = 1.5418 Å) radiation. The crystals were monoclinic space group Pz_1 with the cell parameters $a = 28.074(10)$; $b = 11.287(5)$; $c = 23.654(3)$; $\beta = 117.100(10)$; $V = 6672(3)$ Å, $Z = 4$, and diffracted up to 69.91°. The structure was solved using SHELXS-86 and refined using SHELXS-93. The hydrogens were refined as riding over the heavier atoms. Final R-factor is 0.0955 ($R_w = 0.2562$) for 5256 observed reflections with $F_o \geq 4\sigma(F_o)$. (a) Sheldrick, G. M. *Crystallographic Computing 3*; Oxford University Press: Oxford, U.K., 1985; p 175. (b) Sheldrick, G. M. SHELXS 93; *Program for Crystal Structure Determination*; University of Gottingen: Gottingen, Germany, 1993.

(16) (a) Venkatachalam, C. M. *Biopolymers* **1968**, *6*, 1425−1436. (b) Toniolo, C.; Benedetti, E. *Trends Biochem. Sci.* **1991**, *16*, 350−353. (c) Benedetti, E.; Di Blasio, B.; Pavone, V.; Pedone, C.; Toniolo, C.; Crisma, M. *Biopolymers* **1992**, *32*, 453−456.

(17) (a) Richardson, J. S.; Richardson, D. C. *Science* **1988**, *240*, 1648−1652. (b) Dasgupta, S.; Bell, J. A. *Int. J. Pept. Protein Res.* **1993**, *41*, 499−511. (c) Forood, B.; Feliciano, E. J.; Nambiar, K. P. *Proc. Natl. Acad. Sci. U.S.A.* **1993**, *90*, 838−842. (d) Zhou, H. X.; Lyu, P.; Wemmer, D. E.; Kallenbach, N. R. *Proteins: Struct., Funct., Genet.* **1994**, *18*, 1−7. (e) Doig, A. J.; Baldwin, R. L. *Protein Sci.* **1995**, *4*, 1325−1336. (f) Aurora, R.; Rose, G. D. *Protein Sci.* **1998**, *7*, 21−38.